ARTICLES
PUBLISHED ONLINE: 10 FEBRUARY 2013 | DOI: 10.1038/NPHYS2540
nature physics

Linked attosecond phase interferometry for molecular frame measurements

J. B. Bertrand[1], H. J. Wörner[2], P. Salières[3], D. M. Villeneuve[1]* and P. B. Corkum[1]

High-harmonic spectroscopy uses attosecond techniques to measure single-atom or molecule photorecombination cross-sections. Whereas the amplitude of the extreme-ultraviolet light is easily measurable, the phase is more challenging to access. However, the phase contains information necessary for tomographic imaging of the molecular orbital wavefunction with attosecond–ångström resolution. Present techniques cannot simultaneously measure the phase as a function of molecular angle and photon frequency, which is necessary for a full reconstruction of the wavefunction. We overcome this limitation with an all-optical method that does not require any *ad hoc* assumptions about the phase. We apply it to record the full phase map of aligned bromine molecules relative to reference xenon atoms. It allows us to resolve, both spectrally and angularly, the participation of multiple molecular orbitals, and infer a phase of ionization. This method opens a path to time-resolved molecular orbital tomography.

The high-harmonic generation (HHG) process is composed of three steps: ionization, propagation and photorecombination[1]. Each step contributes an amplitude and a phase to the emitted field $E_{\mathrm{Mol}}(q,\theta) = |D_{\mathrm{Mol}}(q,\theta)|e^{i\Phi_{\mathrm{Mol}}(q,\theta)}$. Here, q is the harmonic order of the emission, and θ is the molecular alignment angle. HHG forms the basis for high-harmonic spectroscopy[2–5]. The phase of the HHG emission contains information about the attosecond synchronization of electron recollision dynamics[6], the instantaneous ionization potential[7], the photorecombination dipole moment[8] and the role of a possible ionization phase[9,10]. Combined with the recently developed coherent detection of chemical reactions[11], knowledge of both amplitude and phase in the molecular frame gives access to the attosecond emission from molecules undergoing chemical dynamics. In particular, knowledge of the recombination phase is necessary for tomographic imaging of the molecular orbital wavefunction[12–15].

As illustrated in Fig. 1, in molecules, the phase $\Phi_{\mathrm{Mol}}(q,\theta)$ is a function of harmonic order q and molecular alignment angle θ. The phase is measured at present by methods developed in attosecond physics—RABBIT (reconstruction of attosecond beating by interference of two-photon transitions[16]) and FROG-CRAB (frequency-resolved optical gating for complete reconstruction of attosecond bursts[17])—by using a synchronized infrared laser field to couple adjacent harmonics in the photoelectron spectrum. These techniques measure the derivative of the spectral phase, and cannot compare the phase between different targets or as a function of molecular angle. A self-referencing spectral interferometry approach[14], where the HHG signal from an imperfectly aligned ensemble of molecules is exploited, determines the angular variation of the phase but leaves the harmonic-order dependence undetermined.

In keeping with the traditions in the field of optical measurement, we call our method by an acronym that is also the name of a small animal. LAPIN (French for rabbit; linked attosecond phase interferometry) is a two-step procedure. A two-source interferometer measures the phase versus molecular angle, $\Phi_{\mathrm{Mol}}(\theta;q)$, and the HHG spectrum of the aligned target molecule mixed with a reference atom is recorded. Each of these steps has been previously demonstrated[9,18–20]. The difficulty until now was the lack of coupling between the two coordinates q and θ of the two-dimensional phase $\Phi_{\mathrm{Mol}}(q,\theta)$. We show that by combining

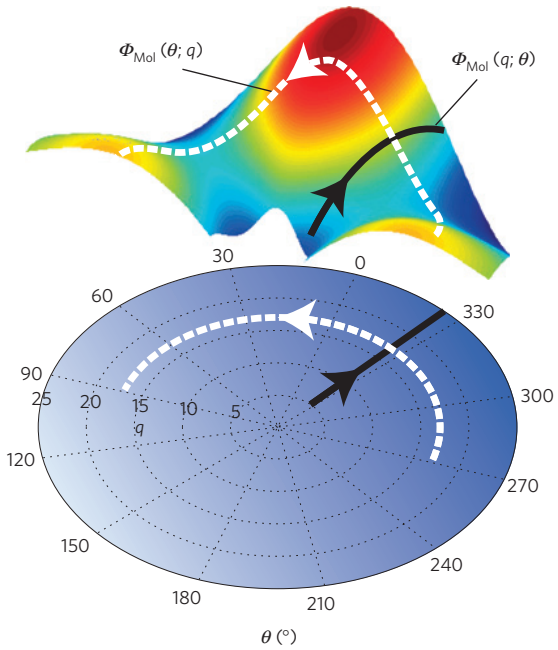

Figure 1 | In aligned molecules, the high-harmonic spectral phase $\Phi_{\mathrm{Mol}}(q,\theta)$ is a function of both harmonic order q and molecular alignment angle θ with respect to the driving laser field polarization axis (linear). Existing techniques can only measure one-dimensional cuts, either the harmonic phase $\Phi_{\mathrm{Mol}}(q;\theta)$ (black line), or the angular phase $\Phi_{\mathrm{Mol}}(\theta;q)$ (white dashed line). Here, we measure the two-dimensional phase $\Phi_{\mathrm{Mol}}(q,\theta)$ relative to that of a reference atom $\Phi_{\mathrm{Ref}}(q)$.

[1]Joint Attosecond Science Laboratory, National Research Council of Canada and University of Ottawa, 100 Sussex Drive, Ottawa K1A 0R6, Canada, [2]Laboratorium für physikalische Chemie, ETH Zürich, Wolfgang-Pauli-Strasse 10, 8093 Zürich, Switzerland, [3]CEA-Saclay, DSM, Service des Photons, Atomes et Molécules, 91191 Gif sur Yvette, France. *e-mail: david.villeneuve@nrc.ca.

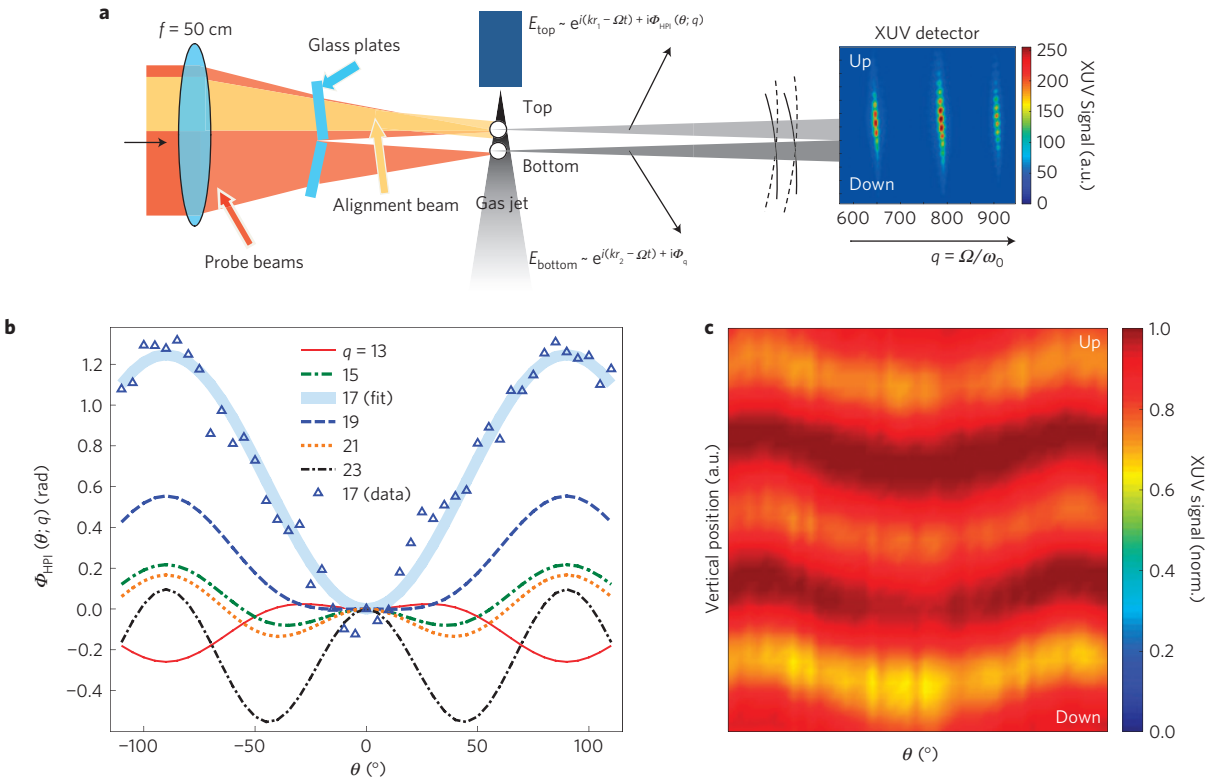

Figure 2 | Spectral harmonic phase interferometry of aligned Br_2 molecules. a, Two XUV sources created in a supersonic gas jet interfere in the far field (XUV detector). We laser-align the molecules in the top source and observe the movement of the interference fringes as a function of alignment angle θ, providing a measurement of the high-harmonic spectral phase $\Phi_{\mathrm{HPI}}(\theta;q)$. **b**, $\Phi_{\mathrm{HPI}}(\theta;q)$ for harmonic orders $q=13$–23 (cutoff). **c**, The measured vertical motion of fringes for $q=17$ as the molecule is rotated from −100° to 100°. The distance between two bright fringes (dark red) corresponds to 2π in phase (see Supplementary Section SI.B for details).

these two measurements, we can unequivocally determine the two-dimensional molecular phase $\Phi_{\mathrm{Mol}}(q,\theta)$ relative to that of a reference atom $\Phi_{\mathrm{Ref}}(q)$. By making the phase measurement relative to a reference atom, we remove the strong atto-chirp[6] that is measured by RABBIT (ref. 16), giving a more accurate measure of the molecular phase. On the other hand, the loss of the atto-chirp information means that the attosecond pulse shape cannot be reconstructed. We apply LAPIN to aligned Br_2 molecules and use xenon as reference atoms.

In the first step, we perform two-source harmonic phase interferometry[9] (HPI). As illustrated in Fig. 2a, we obtain two identical extreme-ultraviolet (XUV) sources by spatially splitting the incoming laser beam using refractive elements placed between the focusing mirror and the gas jet[18] (see Supplementary Section SI for experimental details). Using a thin gas jet allows us to minimize propagation effects and, therefore, to measure the single-molecule response at the XUV detector[5]. The peak intensity of the fundamental pulse in each source is estimated to be $1.5\times10^{14}\,\mathrm{W\,cm^{-2}}$, and the two sources are separated vertically by approximately 150 μm in the gas jet. We impulsively laser-align[21] only the molecules in the top source using a non-ionizing and stretched (130 fs, $3\times10^{13}\,\mathrm{W\,cm^{-2}}$) laser pulse that arrives 0.5 ps earlier to provide prompt molecular alignment. The molecular alignment angle is varied by rotating the alignment pulse polarization with respect to the two-source probe; all polarizations are linear.

The electromagnetic interference between the emitted fields from the top source with aligned (E_{top}) and the bottom source with randomly aligned (E_{bottom}) molecules creates fringes in the far field at the XUV detector, shown in Fig. 2a. Varying the molecular angle, in the top source alone, causes the fringes to move up or down. The variation of the fringe position with molecular angle determines the angular phase for each harmonic, $\Phi_{\mathrm{HPI}}(\theta;q)$. See Supplementary Section SI.B for the definition of the sign convention.

For $q=17$, the fringe displacement and the corresponding phase variation are shown respectively in Fig. 2c,b. The distance between two bright fringes (dark red) is 2π in phase. We arbitrarily choose $\Phi_{\mathrm{HPI}}(\theta=0°;q)=0$ because no connection is made between adjacent harmonics in this measurement. Another approach, exploiting the interference between partially aligned molecules, also gives access to the angular phase[14]. However, it requires some assumptions about the functional form of the rotational wave packet versus time, and it also needs a phase retrieval algorithm.

In the second step, we generate XUV radiation in a mixture of Br_2 molecules and xenon reference atoms. We use the latter as a local oscillator to connect the phase of the Br_2 emission between adjacent harmonics, $\Phi_{\mathrm{Mol}}(q;\theta)$. We prepare a gas mixture with a molar ratio $r\approx0.2{:}1$ of Xe atoms to Br_2 molecules. In Fig. 3a, we show the measured XUV signal $S_{\mathrm{Mix}}(q,\theta,r)$ from this gas mixture, and in Fig. 3b the signal $S_{\mathrm{Mol}}(q,\theta)$ from Br_2 alone, the density of Br_2 molecules being the same in both cases (see Supplementary Section SI for details). All measured signals are normalized according to $S_{\mathrm{Mol}}(q,\theta=0°)=1$. As the signal intensity with the mixed gases is ∼7 times weaker than for pure Br_2 alone, we infer strong destructive interference between the emission of the two species. This even leads to a reversal of the signal angular modulation as seen for harmonic order $q=19$.

The bromine molecules are entrained in a helium carrier gas in the pulsed valve gas expansion. Owing to helium's high ionization potential of 24.6 eV, the helium gas by itself provides no HHG signal. We can add ∼4% by pressure of xenon to the

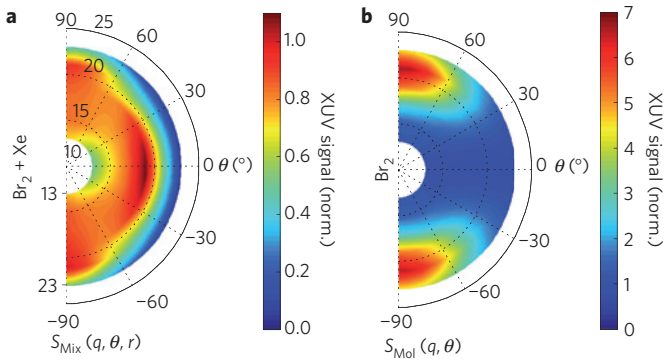

Figure 3 | Mixed-gases interferometry results. a, Measured HHG signal $S_{Mix}(q,\theta)$ from a gas mixture of aligned Br_2 molecules and reference Xe atoms (ratio $r \approx 1{:}0.2$). **b**, $S_{Mol}(q,\theta)$ from aligned Br_2 molecules alone. All measured signals are normalized choosing $S_{Mol}(q,\theta=0°)=1$. The polarization of the HHG (probe) driving laser field is fixed (linear along $\theta=0°$) and the molecular alignment angle θ is varied by rotating the polarization (also linear) of the prompt laser-alignment pump beam.

Table 1 | Relative emission amplitude $r\sqrt{S_{Ref}(q)/S_{Mol}(q,\theta=0°)}$ of the reference atom, as determined by the LAPIN procedure.

Harmonic order	13	15	17	19	21	23
Relative amplitude	0.66	0.48	0.72	1.55	1.64	1.37

All measured signals are normalized to $S_{Mol}(q,\theta=0°)=1$.

helium, without affecting the gas expansion. However, we cannot directly measure the HHG spectrum from the reference atom alone $S_{Ref}(q)$, as done in other experiments[19,20], because the pulsed valve operation and thereby the gas expansion are different without Br_2 vapours. Instead, we separately record the HHG spectra of bromine molecules alone $[S_{Mol}(q,\theta)]$ and of the gas mixture $[S_{Mix}(q,\theta)]$. This removes the difficulty in matching gas expansion conditions with and without Br_2 molecules, and relieves the necessity to know the precise ratio of gas pressures r: our fitting procedure uniquely determines the reference atom contribution. We express the mixed-gases emission as the coherent sum of the emission from each species[20]:

$$S_{Mix}(q,\theta,r) = S_{Mol}(q,\theta) + r^2 S_{Ref}(q) + 2r\sqrt{S_{Ref}(q)}\sqrt{S_{Mol}(q,\theta)}\cos\Delta\Phi_{Mix}(q,\theta) \quad (1)$$

Here, we define $\Delta\Phi_{Mix}(q,\theta) = \Phi_{Mol}(q,\theta) - \Phi_{Ref}(q)$ as the phase difference between the electromagnetic emission from the aligned molecules $E_{Mol}(q,\theta)$ and the reference atom $E_{Ref}(q)$. We know all quantities except for $r^2 S_{Ref}(q)$ and $\Delta\Phi_{Mix}(q,\theta)$. For each harmonic order q, we have 21 measurements corresponding to different molecular angles θ. Therefore, there is sufficient information to determine both $r^2 S_{Ref}(q)$ and $|\Delta\Phi_{Mix}(q,\theta)|$, provided that we parameterize the phase.

In mixed-gases interferometry, an ambiguity on the phase arises because $\cos\Delta\Phi_{Mix}(q,\theta)$ is symmetric around $\Delta\Phi_{Mix}(q,\theta)=0$. Two solutions, $\pm\Delta\Phi_{Mix}(q,\theta)$, can satisfy equation (1), thereby accessing only $|\Phi_{Mol}(q,\theta) - \Phi_{Ref}(q)|$. Previous work[19] assumed a direction of the phase difference $\Delta\Phi_{Mix}(q,\theta)$ to extract it. Here, we can use the redundant information provided by the spectral phase interferometry measurement (Fig. 2) to lift the sign ambiguity of the phase. For this purpose, we combine both experimental measurements into a global fitting procedure described in Supplementary Section SII.B.

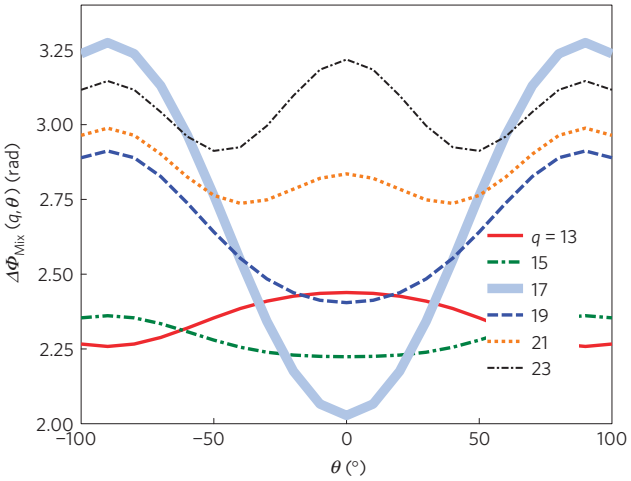

Figure 4 | Experimentally determined relative phase $\Delta\Phi_{Mix}(q,\theta)$ between the molecule and reference atom. The mixed-gases (Fig. 3) and harmonic phase interferometry (Fig. 2) measurements are combined in the LAPIN procedure.

The relative signal amplitude from the reference atom $r\sqrt{S_{Ref}(q)/S_{Mol}(q,\theta=0°)}$ and phase $\Delta\Phi_{Mix}(q,\theta)$, determined by the LAPIN fitting procedure, are respectively shown in Table 1 and Fig. 4. For all harmonic orders q, the variation of $\Delta\Phi_{Mix}(q,\theta)$ with molecular angle resembles closely the phase measured by harmonic phase interferometry $\Phi_{HPI}(\theta;q)$ in Fig. 2b. In both cases, the low harmonics ($q=13$, 15) modulate less, the strongest modulation occurs at $q=17$ and the cutoff harmonics ($q=21$, 23) show a double modulation.

We have now demonstrated the LAPIN method, and its ability to measure the full two-dimensional spectral amplitude and phase of attosecond emission from aligned molecules relative to that of reference atoms. This XUV photonics method is important for molecular imaging[15] as it extracts only contributions to HHG that are target-specific (as opposed to laser-specific), such as the photorecombination dipole. We now proceed to interpret the measurement and to compare it with single-molecule quantum chemistry predictions. We will extract both the amplitude and phase of the recombination dipole moment, using the retrieved relative electromagnetic phase $\Delta\Phi_{Mix}(q,\theta)$ and amplitude $r\sqrt{S_{Ref}(q)/S_{Mol}(q,\theta=0°)}$.

We recall that all three HHG steps contribute to the phase: ionization (I), propagation (P) and photorecombination (R). As the same laser field is used to simultaneously generate harmonics in Br_2 and Xe in mixed-gases interferometry, the phase difference ($\Delta\Phi_P(q)$) associated with the acceleration of the electron in the continuum essentially cancels out. However, a contribution associated with the difference in ionization potential ($\Delta I_p = -1.58$ eV) between Br_2 ($I_{p,HOMO} = 10.55$ eV) and Xe ($I_p = 12.13$ eV) remains: $\Delta\Phi_P(q) = -\Delta I_p \tau_q$ (refs 13,22,23), with τ_q being the calculated classical electron excursion time associated with the short trajectory harmonic order q. As a result, we can extract a relative phase $\Delta\Phi_{Mol-Ref}(q,\theta)$ between the molecule (The highest occupied molecular orbital, HOMO, is the molecular reference point) and the reference atom that includes contributions from both the photorecombination (R) and possibly the ionization (I) steps[9,10]:

$$\Delta\Phi_{Mol-Ref}(q,\theta) = \Delta\Phi_{Mix}(q,\theta) - \Delta\Phi_P(q) = \Delta\Phi_R(q,\theta) + \Delta\Phi_I(q,\theta) \quad (2)$$

At this point we could also remove the recombination phase of the reference xenon atom, which we calculated and show

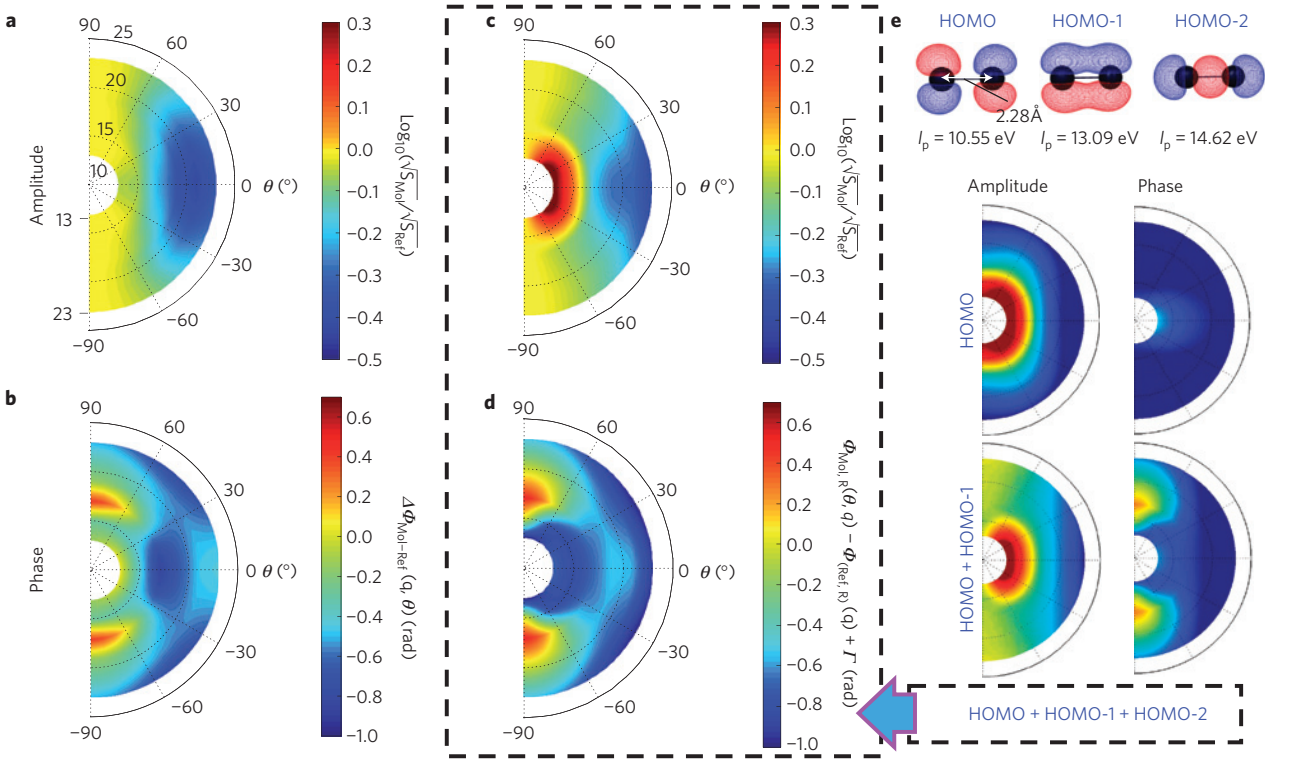

Figure 5 | Experimentally determined molecular frame amplitude and phase compared with model calculations. a,**b**, LAPIN-retrieved relative amplitude $\sqrt{S_{\mathrm{Mol}}(q,\theta)/S_{\mathrm{Ref}}(q)}$ (**a**) and phase $\Delta\Phi_{\mathrm{Mol-Ref}}(q,\theta)$ (**b**) between the emission from Br_2 molecules and reference Xe atoms. **c**,**d**, Calculated relative amplitude (**c**) and phase contribution (**d**) from multiple orbitals altogether (HOMO + HOMO-1 + HOMO-2). **e**, We progressively add the coherent contributions from each orbital to the total amplitude and phase. The theoretical calculations (**c**)-(**e**) are relative to the same calculations for xenon atoms, and hence can be directly compared to the experiment. For clarity, all amplitudes are normalized to the values at $\theta = 90°$ ((**a**),(**c**)) for each harmonic order (see Supplementary Section SIII for unnormalized plots). All amplitudes and phases are, respectively, shown using common colour scales.

in Supplementary Section SII.A. Instead, we will leave out the experimentally determined amplitude and phase of bromine relative to xenon (see Fig. 5a,b), and include the calculated xenon recombination amplitude and phase in the theoretical model, which we shall describe next.

At the laser intensity $I_{\mathrm{probe}} = 1.5 \times 10^{14}\,\mathrm{W\,cm^{-2}}$ used in the experiment, multiple molecular orbitals of Br_2 (HOMO, HOMO-1 and HOMO-2) can significantly contribute to HHG (refs 9,24,25). Indeed, a strong-field approximation calculation[26] on atoms with $I_{\mathrm{p,HOMO}} = 10.55$ eV, $I_{\mathrm{p,HOMO-1}} = 13.09$ eV and $I_{\mathrm{p,HOMO-2}} = 14.62$ eV shows that, although HOMO emits the strongest for $q \leq 15$, the contributions from HOMO-1 and HOMO-2 become dominant for $q \geq 17$ (see Supplementary Fig. S7b). To simulate the experiment, we coherently add the contributions from HOMO, HOMO-1 and HOMO-2 along the lines of refs 9,25, using molecular photorecombination dipoles obtained by quantum scattering calculations[27,28] (see Supplementary Section SIII for details on the theoretical model). To be consistent with our definition of $\Delta\Phi_{\mathrm{Mol-Ref}}(q,\theta)$ retrieved experimentally (see equation (2)), we also take HOMO as the molecular reference point and include the ionization potential differences relative to HOMO when calculating the expected photorecombination dipole relative phase $\Delta\Phi_{\mathrm{R}}(q,\theta) = \Phi_{\mathrm{Mol,R}}(q,\theta) - \Phi_{\mathrm{Ref,R}}(q)$ (see Supplementary Equations S10–S12). In Fig. 5c–e, we show the progressive contribution of each orbital to the total relative amplitude (Fig. 5c) and phase (Fig. 5d).

The calculated amplitude and phase in Fig. 5c,d are in good agreement with the LAPIN experimental results in Fig. 5a,b. Our calculations reveal that HOMO-1 is responsible for the amplitude and phase mainly peaking at $\theta = 90°$ (see Fig. 5e lower panel). An amplitude minimum in the vicinity of $q = 21$ and $\theta = 0°$, accompanied by a rapid local phase variation with increasing q, is observed experimentally. The position of this minimum ($q = 21$) is consistent with the two-centre interference model[29]; a similar feature around $q = 23$ was also observed in the recombination dipole of aligned CO_2 measured by the RABBIT technique[8], and around $q = 33$ (50 eV) measured by the generalized orbital tomography approach[14], Br_2 and CO_2 having the same ordering of valence molecular orbitals. However, the dependence of that spectral feature on laser intensity[9] and wavelength[25] in CO_2 instead supports the participation of multiple orbitals[24]. Here, our calculations in Fig. 5c–e qualitatively reproduce the spectral minimum and rapid phase variation observed experimentally in Fig. 5a,b: they would also originate from the interplay of multiple orbitals. Less good agreement between experiment and theory is visible at lower harmonic orders, suggesting that our model based on the strong-field approximation may overestimate the relative contribution from the HOMO.

For quantitative agreement between experiment and theory phases (Fig. 5b,d), we need to add an overall constant $\Gamma \approx -0.9\pi$ to the calculated recombination phase $\Phi_{Mol,R}(q,\theta) - \Phi_{Ref,R}(q)$. On the basis of equation (2), this suggests an additional constant phase difference between the emission from HOMO and xenon, $\Gamma \approx -0.9\pi$. Although the concept of an ionization phase is not yet fully understood[9,10], $\Delta\Phi_I \approx -0.9\pi$ would explain the overall shift between the experiment and the model. As a result, comparing LAPIN measurements to our model allows us to report an additional, previously unaccounted for, phase difference between the emission of two species in mixed-gases experiments[19,20,23]. This needs to be further investigated by more detailed modelling, which could include multielectron attosecond dynamics and sub-cycle laser-driven population evolution of the electron–hole first created

by ionization[9,10]. Our results on Br_2 support previous results in CO_2 where no ionization phase is observed between the XUV emission from different molecular orbitals[9].

We have combined two all-optical techniques, namely two-source harmonic phase and mixed-gases interferometries, allowing us to first solve for the full two-dimensional (q, θ) molecular high-harmonic photorecombination dipole amplitude and phase relative to those of a reference atom. Accessing these full quantities is especially important for the development of single-molecule tomographic imaging by HHG (ref. 12–15). Although we demonstrated the LAPIN technique using 30-fs laser pulses, unlike RABBIT (ref. 16), it will work for few-cycle pulses where individual harmonics are not resolved. Moreover, it is *in situ*: it uses a single gas jet and an XUV spectrometer, whereas present techniques require a second gas jet and a photoelectron spectrometer[16,17]. LAPIN is applicable to any molecular systems that can be expanded in the gaseous phase; these include: aligned[21], three-dimensionally aligned[30] and oriented[31] polyatomic molecules. As its retrieval procedure directly measures the full phase map relative to the reference atom, LAPIN offers the opportunity to benchmark new theoretical models[2] and extend them to larger molecules. The combination of LAPIN and time-resolved homodyne high-harmonic spectroscopy[11] now provides all necessary information for dynamical tomographic imaging of chemical reactions. This procedure will surely bring new insights into single-molecule electronic dynamics underlying photochemical processes such as photosynthesis[32,33].

Received 20 June 2012; accepted 24 December 2012; published online 10 February 2013

References

1. Corkum, P. B. & Krausz, F. Attosecond science. *Nature Phys.* **3,** 381–387 (2007).
2. Le, A-T., Lucchese, R. R., Tonzani, S., Morishita, T. & Lin, C. D. Quantitative rescattering theory for high-order harmonic generation from molecules. *Phys. Rev. A* **80,** 013401 (2009).
3. Popmintchev, T., Chen, M-C., Arpin, P., Murnane, M. M. & Kapteyn, H. C. The attosecond nonlinear optics of bright coherent X-ray generation. *Nature Photon.* **4,** 822–832 (2010).
4. Frolov, M. V., Manakov, N. L., Sarantseva, T. S. & Starace, A. F. Analytic confirmation that the factorized formula for harmonic generation involves the exact photorecombination cross section. *Phys. Rev. A* **83,** 043416 (2011).
5. Shiner, A. D. *et al.* Probing collective multi-electron dynamics in xenon with high-harmonic spectroscopy. *Nature Phys.* **7,** 464–467 (2011).
6. Mairesse, Y. *et al.* Attosecond synchronization of high-harmonic soft X-rays. *Science* **302,** 1540–1543 (2003).
7. Wörner, H. J., Bertrand, J. B., Corkum, P. B. & Villeneuve, D. M. High-harmonic homodyne detection of the ultrafast dissociation of BR_2 molecules. *Phys. Rev. Lett.* **105,** 103002 (2010).
8. Boutu, W. *et al.* Coherent control of attosecond emission from aligned molecules. *Nature Phys.* **4,** 545–549 (2008).
9. Smirnova, O. *et al.* High harmonic interferometry of multi-electron dynamics in molecules. *Nature* **460,** 972–977 (2009).
10. Mairesse, Y. *et al.* High harmonic spectroscopy of multichannel dynamics in strong-field ionization. *Phy. Rev. Lett.* **104,** 213601 (2010).
11. Wörner, H. J., Bertrand, J. B., Kartashov, D. V., Corkum, P. B. & Villeneuve, D. M. Following a chemical reaction using high-harmonic interferometry. *Nature* **466,** 604–607 (2010).
12. Itatani, J. *et al.* Tomographic imaging of molecular orbitals. *Nature* **432,** 867–871 (2004).
13. Haessler, S. *et al.* Attosecond imaging of molecular electronic wavepackets. *Nature Phys.* **6,** 200–2006 (2010).
14. Vozzi, C. *et al.* Generalized molecular orbital tomography. *Nature Phys.* **7,** 822–826 (2011).
15. Haessler, S., Caillat, J. & Salières, P. Self-probing of molecules with high harmonic generation. *J. Phys. B* **44,** 203001 (2011).
16. Paul, P. M. *et al.* Observation of a train of attosecond pulses from high harmonic generation. *Science* **292,** 1689–1692 (2001).
17. Mairesse, Y. & Quéré, F. Frequency-resolved optical gating for complete reconstruction of attosecond bursts. *Phys. Rev. A* **71,** 011401 (2005).
18. Zhou, X. *et al.* Molecular recollision interferometry in high harmonic generation. *Phys. Rev. Lett.* **100,** 073902 (2008).
19. McFarland, B. K., Farrell, J. P., Bucksbaum, P. H. & Gühr, M. High-order harmonic phase in molecular nitrogen. *Phys. Rev. A* **80,** 033412 (2009).
20. Wagner, N. *et al.* Extracting the phase of high-order harmonic emission from a molecule using transient alignment in mixed samples. *Phys. Rev. A* **76,** 061403 (2007).
21. Stapelfeldt, H. & Seideman, T. Aligning molecules with strong laser pulses. *Rev. Mod. Phys.* **75,** 543–557 (2003).
22. Lewenstein, M., Balcou, P., Ivanov, M. Y., L'Huillier, A. & Corkum, P. B. Theory of high-harmonic generation by low-frequency laser fields. *Phys. Rev. A* **49,** 2117–2132 (1994).
23. Kanai, T., Takahashi, E. J., Nabekawa, Y. & Midorikawa, K. Destructive interference during high harmonic generation in mixed gases. *Phys. Rev. Lett.* **98,** 153904 (2007).
24. McFarland, B. K., Farrell, J. P., Bucksbaum, P. H. & Gühr, M. High harmonic generation from multiple orbitals in N_2. *Science* **322,** 1232–1235 (2008).
25. Wörner, H. J., Bertrand, J. B., Hockett, P., Corkum, P. B. & Villeneuve, D. M. Controlling the interference of multiple molecular orbitals in high-harmonic generation. *Phys. Rev. Lett.* **104,** 233904 (2010).
26. Yakovlev, V. S., Ivanov, M. & Krausz, F. Enhanced phase-matching for generation of soft X-ray harmonics and attosecond pulses in atomic gases. *Opt. Express* **15,** 15351–15364 (2007).
27. Gianturco, F. A., Lucchese, R. R. & Sanna, N. Calculation of low-energy elastic cross sections for electron-CF_4 scattering. *J. Chem. Phys.* **100,** 6464–6471 (1994).
28. Natalense, A. P. P. & Lucchese, R. R. Cross section and asymmetry parameter calculation for sulphur 1s photoionization of SF_6. *J. Chem. Phys.* **111,** 5344–5348 (1999).
29. Lein, M., Hay, N., Velotta, R., Marangos, J. & Knight, P. Role of the intramolecular phase in high-harmonic generation. *Phys. Rev. Lett.* **88,** 183903 (2002).
30. Lee, K. F., Villeneuve, D. M., Corkum, P. B., Stolow, A. & Underwood, J. G. Field-free three-dimensional alignment of polyatomic molecules. *Phys. Rev. Lett.* **97,** 173001 (2006).
31. De, S. *et al.* Field-free orientation of CO molecules by femtosecond two-colour laser fields. *Phys. Rev. Lett.* **103,** 153002 (2009).
32. Wörner, H. J. *et al.* Conical intersection dynamics in NO_2 probed by homodyne high-harmonic spectroscopy. *Science* **334,** 208–212 (2011).
33. Whitaker, B. J. Shining light on diabolic points. *Science* **334,** 187–188 (2011).

Acknowledgements

The authors gratefully acknowledge financial support from NSERC, CIPI, AFOSR and the NRC-CEA agreement.

Author contributions

J.B.B., H.J.W., P.S., D.M.V. and P.B.C. conceived the experiment and helped prepare the manuscript. J.B.B. and H.J.W. performed all experiments. J.B.B. and D.M.V. developed the LAPIN algorithm. J.B.B. did all data analysis and calculations, prepared all figures and led the writing of the manuscript.

Additional information

Supplementary information is available in the online version of the paper. Reprints and permissions information is available online at www.nature.com/reprints. Correspondence and requests for materials should be addressed to D.M.V.

Competing financial interests

The authors declare no competing financial interests.